MICS JOURNAL

Mathematics-in-Industry Case Studies Journal, Volume 1, pp. 9-23 (2008)

On the stability of sheared menisci in Hele-Shaw cells

B.S. Tilley [*] J. Billingham [†] F. Hendriks [‡]

Abstract. In this paper, we begin to consider viscous and wettability effects in the interfacial stability of fluid dynamic bearings in hard-disk drives. As a canonical problem, the linear stability of a sheared meniscus between two parallel plates is investigated when inertial effects are neglected. Through an asymptotic analysis, we prescribe the appropriate boundary conditions on the interfacial contact line which regularizes the contact-line singularity due to the application of no-slip. We find that for sufficiently large capillary numbers, two neutrally stable modes are always found, and the next least stable modes correspond to temporally-decaying standing waves, whose average speed is the same as the average base-state flow velocity. Although all modes are stable, we discuss the impact of these results when inertial effects are pertinent.

Keywords. linear stability theory, oil-air interface, bearing hard disk drive

1 Introduction

Recently, the use of fluid dynamic bearing spindle motors in hard-disk drive applications has been widespread, due to lowering acoustical noise, minimizing Non Repeatable Runout (NRRO) and improving reliability [1]. Figure 1a shows a schematic of a sample disk drive, and a simplified cross-section of the stator and the rotor. Typical spatial dimensions are shown in the figure. Characteristic rotation rates for server drives are 10,000 and 15,000 rpm, while laptop drives may be 4,500 and 7,200 rpm. The bearing fluid is held by capillary pressures, thus any instability of the interface could lead to ejection of the fluid and mechanical failure. Rotation rates have increased and it is important to find the critical capillary and Weber numbers at which the surface becomes unstable. The focus of this paper is on the stability of the meniscus region during operation. Note that the rotor and stator have smooth surfaces, unlike those found near the bearing region where

[*]Franklin W. Olin College Engineering, Olin Way, Needham, Maine, 02492, United States of America, tilley@olin.edu

[†]School of Mathematical Sciences, University of Nottingham, University Park, Nottingham, NG7 2RD, United Kingdon, john.billingham@nottingham.ac.uk

[‡]Hitachi Global Storage Technologies, 3403 Yerba Buena Road, San Jose, California, 95135, United States of America, ferdi.hendriks@hitachigst.com

pressures of several atmospheres are generated (see Hendriks *et al.* [3]). In Hendriks *et al.*, the pressure field does not significantly change as the axial coordinate approaches the interface, much as in the assumption used in Hele-Shaw flows (see [4]). In this work, we are interested in the pressure field near the interfacial region, and it is not clear *a priori* if pressure fluctuations are significant. We assume here that any disturbance pressures from the fluid-dynamic bearing region are negligible.

Note from Table 1, hydrostatic pressures are small compared to the capillary pressures (i.e. $Bo \approx 1/50$). Hence, the tilt of the axis, as shown in Figure 1a, need not be considered. Further, since we are interested in gap thicknesses that are smaller than the stator radius ($d \ll R$), we neglect centrifugal and Coriolis effects. Thus Taylor cells cannot occur. This suggests consideration of the planar problem shown in Figure 1b. The plate located at $x = 0$ is held steady, while the plate at $x = d$ translates with a speed U_o. Note that this problem provides a cleaner study of the role viscous and wettability effects play in the response of the interface to infinitesimal disturbances.

The inviscid limit of this case, or the zero capillary number limit has been considered by Walker *et al.* [2]. In this limit, normal and tangential viscous stresses are ignored, and any contact-line dynamics are not considered. Further, Walker *et al.* [2] restricted the linear stability analysis to disturbances whose wavespeed moves at the average speed $c_r = U_o/2$ of the Couette flow. In their study, the critical wavenumber of the disturbance centers near $k \approx 2\pi/d$, or with a wavelength equal to the gap length and based on the Weber number $We = \rho U_o^2 d/\sigma$, where ρ is the fluid density and σ is its surface tension. In this application, $We \approx 90$, which suggests from [2] that a wide band of unstable modes is possible under normal operation. However, any inviscid analysis must neglect tangential stresses at the fluid boundaries, such as wettability effects and viscous stresses. In this application, they appear to play a role in the propagation speed of the disturbance. In what follows, we consider the $Re \to 0$ limit, and find that this system remains stable for all of the eigenvalues found, however, the most dangerous modes (or least stable modes) have wavespeeds that differ from the average fluid speed.

The paper is organized in the following manner. In Section 2, we develop the linear stability theory for the oil-air interface (OAI) problem in a Cartesian, or slot geometry. A finite difference method for the solution to the linear problem is discussed in Section 3. From this analysis, we find that for finite capillary numbers, two neutrally stable modes appear independent of the wavenumber. In addition, modes with sufficiently small wavelengths that propagate at the average speed of the plates for small capillary numbers undergo a Hopf bifurcation as the capillary number is increased for sufficiently large wavenumbers.

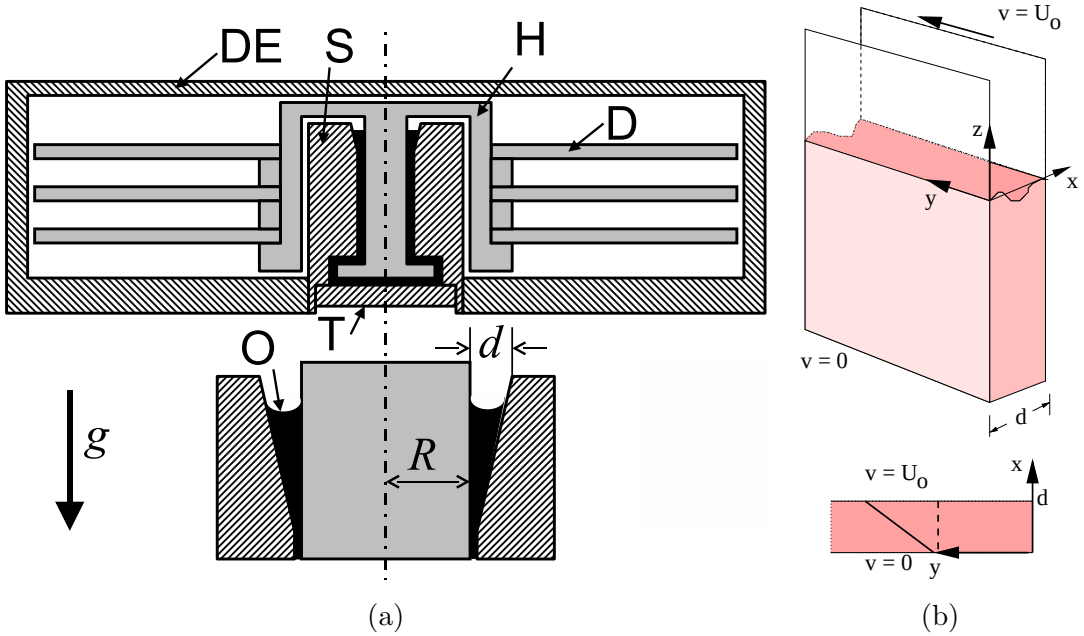

Figure 1: *(a) A simplified cross-section of a disk drive with a rotating shaft. DE: Disk enclosure, S: stator, H: hub, O: oil, T: thrust plate, g: gravitational acceleration, d: oil/air interface width (gap width), R: shaft radius. (b) Idealized problem under consideration of a sheared meniscus in a Hele-Shaw cell.*

2 Problem Formulation

Consider an incompressible viscous fluid (the 'oil') that is confined to the infinite slot between two vertical side walls, one stationary, one moving (see Figure 1b). The fluid does not entirely fill the slot. The domain occupied by the fluid is bounded above by a free surface located at $z = F(x, y, t)$. We use a Cartesian coordinate system, oriented so that the fluid meets the stationary side wall at $x = 0$. The moving wall $x = d$ is translating along the slot in the y direction with speed U_o. We assume that the air above the interface only provides a constant reference pressure on the interface, and its dynamics does not affect the stability.

We use the incompressible Navier-Stokes equations to describe the motion of the fluid,

$$\nabla \cdot \mathbf{u} = 0. \tag{1}$$

$$\rho \left\{ \frac{\partial \mathbf{u}}{\partial t} + (\mathbf{u} \cdot \nabla)\mathbf{u} \right\} = -\nabla p + \mu \nabla^2 \mathbf{u} + \rho \mathbf{g}, \tag{2}$$

where $\mathbf{u} = (u, v, w)$ is fluid velocity at (x, y, z), p is the fluid pressure, ρ is the fluid density, μ is the dynamic viscosity of the fluid, and $\mathbf{g}$ is the gravitational vector.

Dimensional quantities		Dimensionless quantities	
Gap thickness d	200 μm	Aspect Ratio	$\alpha = d/R = 10^{-1}$
Stator radius R	2 mm	Froude Number	$Fr = \frac{(\Omega R)^2}{(gd)} = 5000$
Rotation rate Ω	15,000 rpm	Bond Number	$Bo = \frac{\rho g d^2}{\sigma} = 0.02$
Velocity $U_o = \Omega R$	3 m/s	Reynolds Number	$Re = \frac{\rho U_o d}{\mu} = 60$
Fluid density ρ	900 kg/m^3	Capillary Number	$Ca = \frac{\mu \Omega R}{\sigma} = 1.5$
Fluid dynamic viscosity μ	0.01 Pa· s	Weber Number	$We = ReCa = 90$
Surface tension σ	0.02 N/m	Galileo Number	$Ga = Bo/Ca = 0.013$

Table 1: *Table of dimensional and dimensionless quantities.*

The boundary conditions are the no-slip boundary conditions along the walls[1],

$$\underline{x = 0} : u = v = w = 0 \ , \underline{x = d} : u = w = 0, v = U_o \ . \tag{3}$$

In addition, we assume that the flow far from the interface approaches plane Couette flow

$$\underline{z \to -\infty} : u, w \to 0 \ , v \to U_o x/d \ . \tag{4}$$

At the free surface, we apply the kinematic boundary condition, normal fluid stresses are balanced by capillary stresses, and there are no applied tangential stresses to the fluid at the interface:

$$F_t + uF_x + vF_y - w = 0 \tag{5}$$

$$-p + 2\mu \mathbf{n} \cdot \mathbf{e} \cdot \mathbf{n} = \sigma\kappa \tag{6}$$

$$\mathbf{e} \cdot \mathbf{n} \times \mathbf{n} = \mathbf{0} \tag{7}$$

where $\mathbf{e} = (\mathbf{e}_{i,j})_{3\times 3}$ with $\mathbf{e}_{i,j} = (\partial u_i/\partial x_j + \partial u_j/\partial x_i)/2$ and u_i and x_i are short-hand notation for the (u, v, w) and (x, y, z) is the rate-of-strain tensor of the fluid, $\mathbf{n}$ is the outward unit normal vector to the interface

$$\mathbf{n} = \frac{-F_x\mathbf{x} \ - F_y\mathbf{y} \ + \mathbf{z}}{\sqrt{1 + F_x^2 + F_y^2}} \ ,$$

σ is the surface tension of the oil, $\kappa = \nabla \cdot \mathbf{n}$ and is the mean curvature.

We apply the following scales to the problem, using the notation $[f]$ to denote the scale,

$$[x, y, z] = d \ , \ [u, v, w] = U_o \ , \ [t] = d/U_o \ , \ [p] = \frac{\mu U_o}{d} \ , \ [F] = d \ ,$$

to find the following nondimensional version of our system

$$\frac{\partial u}{\partial x} + \frac{\partial v}{\partial y} + \frac{\partial w}{\partial z} = 0 \ , \tag{8}$$

[1]The nonintegrable stress singularity at the contact lines will be addressed in a later section

$$Re\left(\frac{\partial u}{\partial t}+u\frac{\partial u}{\partial x}+v\frac{\partial u}{\partial y}+w\frac{\partial u}{\partial z}\right)=-\frac{\partial p}{\partial x}+\left(\frac{\partial^2 u}{\partial x^2}+\frac{\partial^2 u}{\partial y^2}+\frac{\partial^2 u}{\partial z^2}\right), \tag{9}$$

$$Re\left(\frac{\partial v}{\partial t}+u\frac{\partial v}{\partial x}+v\frac{\partial v}{\partial y}+w\frac{\partial v}{\partial z}\right)=-\frac{\partial p}{\partial y}+\left(\frac{\partial^2 v}{\partial x^2}+\frac{\partial^2 v}{\partial y^2}+\frac{\partial^2 v}{\partial z^2}\right), \tag{10}$$

$$Re\left(\frac{\partial w}{\partial t}+u\frac{\partial w}{\partial x}+v\frac{\partial w}{\partial y}+w\frac{\partial w}{\partial z}\right)=-\frac{\partial p}{\partial z}-Ga+\left(\frac{\partial^2 w}{\partial x^2}+\frac{\partial^2 w}{\partial y^2}+\frac{\partial^2 w}{\partial z^2}\right), \tag{11}$$

where $Re = U_o d/\nu$, $Bo = \rho g d^2/\sigma$, $Ca = \mu U_o/\sigma$, $Ga = Bo/Ca$ is the Reynolds number, the Bond number, the capillary number, and the Galileo number, respectively. The no-slip boundary conditions become

$$\underline{x=0}: \quad u=v=w=0\ ,\ \underline{x=1}: \quad u=w=0\ , v=1\ , \tag{12}$$

and the far-field condition becomes

$$\underline{z\to-\infty}:\ u,w\to 0\ , v\to x\ . \tag{13}$$

The interfacial conditions (5)-(7) become

$$F_t+uF_x+vF_y-w=0 \tag{14}$$

$$-p+\frac{2}{\sqrt{1+F_x^2+F_y^2}}\left\{w_z-F_y\left(v_z+w_y\right)-F_x\left(u_z+w_x\right)+F_y^2 v_y+F_x^2 u_x+2F_xF_y\left(u_y+v_x\right)\right\}$$
$$=\frac{1}{Ca}\left\{\frac{F_{xx}\left(1+F_x^2\right)+F_{yy}\left(1+F_y^2\right)-2F_xF_yF_{xy}}{\left(1+F_x^2+F_y^2\right)^{3/2}}\right\}\ , \tag{15}$$

$$\left\{\left(u_z+w_x\right)\left(1-F_x^2\right)-F_y(u_y+v_x)+2F_x(w_z-u_x)-F_xF_y(v_y+w_x)\right\} = 0 \tag{16}$$
$$\left\{\left(v_z+w_y\right)\left(1-F_y^2\right)-F_x(u_y+v_x)+2F_y(w_z-v_y)-F_yF_x(u_z+w_x)\right\} = 0\ . \tag{17}$$

2.1 Linearisation around the Basic State

Note that the Couette flow $u=w=0, v=x, p=-Ga\,z$ solves this problem provided that $F=0$ for all x,y with a wetting angle of $\pi/2$. We perform the linear stability theory of this problem about this state with the assumption

$$u = \delta\left\{\hat{U}(x,z)e^{ik(y-ct)} + c.c.\right\} \tag{18}$$
$$v = x + \delta\left\{\hat{V}(x,z)e^{ik(y-ct)} + c.c.\right\} \tag{19}$$
$$w = \delta\left\{\hat{W}(x,z)e^{ik(y-ct)} + c.c.\right\} \tag{20}$$
$$p = -Ga\,z + \delta\left\{\hat{P}(x,z)e^{ik(y-ct)} + c.c.\right\} \tag{21}$$
$$F = \delta\left\{\hat{F}(x)e^{ik(y-ct)} + c.c.\right\}\ , \tag{22}$$

for $\delta \ll 1$. Substituting this Ansatz into (8)-(17) and keeping only the terms which are linear in δ to arrive at the system

$$\hat{U}_x + i\,k\,\hat{V} + \hat{W}_z = 0, \tag{23}$$
$$\hat{U}_{xx} + \hat{U}_{zz} - k^2\hat{U} - \hat{P}_x = ik\,Re\,(x-c)\,\hat{U}, \tag{24}$$
$$\hat{V}_{xx} + \hat{V}_{zz} - k^2\,\hat{V} - ik\hat{P} = Re\left\{\hat{U} + ik\,(x-c)\,\hat{V}\right\}, \tag{25}$$
$$\hat{W}_{xx} + \hat{W}_{zz} - k^2\hat{W} - \hat{P}_z = ik\,Re\,(x-c)\,\hat{W}, \tag{26}$$

on $0 < x < 1$ and $z < 0$, subject to

$$\hat{U} = \hat{V} = \hat{W} = 0 \qquad \text{at } x = 0 \text{ and } x = 1 \text{ for } z < 0, \tag{27}$$
$$\hat{U} \to 0, \quad \hat{V} \to 0, \quad \hat{W} \to 0 \qquad \text{as } z \to -\infty \text{ for } 0 < x < 1, \tag{28}$$
$$i\,k\,(x-c)\hat{F} = \hat{W} \qquad \text{at } z = 0 \text{ for } 0 < x < 1, \tag{29}$$
$$-Ca\left(\hat{P} - 2\hat{W}_z\right) = \hat{F}_{xx} - (Ga + k^2)\hat{F} \qquad \text{at } z = 0 \text{ for } 0 < x < 1, \tag{30}$$
$$\hat{V}_z + ik\hat{W} = \hat{F}_x \qquad \text{at } z = 0 \text{ for } 0 < x < 1, \tag{31}$$
$$\hat{U}_z + \hat{W}_x = ik\,\hat{F} \qquad \text{at } z = 0 \text{ for } 0 < x < 1, \tag{32}$$
$$\hat{F}_x = 0 \qquad \text{at } z = 0,\ x = 0 \text{ and } x = 1. \tag{33}$$

This formulation is incomplete, since it is well-known that prescribing (27), a no slip boundary condition, all the way up to a moving contact line, implicit in (33), which states that the contact angle remains at its static value, leads to a non-integrable singularity in the stress at the contact line (see [5]). There are many ways of dealing with this difficulty, but the simplest is to use a modified boundary condition in a small neighbourhood of the moving contact line, of dimensionless extent ϵ, and specify that the contact angle remains constant, so that (33) remains valid. Then, the contact angle measured some small distance much greater than ϵ from the contact line (the apparent contact angle) is significantly different from the static contact angle because viscous normal stresses in the neighbourhood of the contact line cause significant bending of the interface (see [6]).

We can see how these ideas can be applied to our problem by considering the asymptotic solution in the neighbourhood of a contact line. In this local region, we assume that inertial effects and

hydrostatic effects are negligible ($Re = 0, Ga = 0$). We rescale z on the distance between the plates, and in terms of polar coordinates with origin at $x = z = 0$, with the solid wall, $x = 0$, at $\theta = 0$ and the free surface, $z = 0$, at $\theta = \pi/2$, we can write the linear stability problem as

$$\nabla \cdot \mathbf{U} = -i\,kV, \tag{34}$$

$$\nabla^2 \mathbf{U} - k^2 \mathbf{U} - \nabla P = 0, \tag{35}$$

$$\nabla^2 V - k^2 V + ikP = 0, \tag{36}$$

for $0 < \theta < \pi/2$, where $\mathbf{U} = (U, W)$. Writing the polar components of $\mathbf{U}$ as U_θ and U_r, the local boundary conditions are, at $\theta = \pi/2$,

$$U_\theta = ik(r - c)F, \tag{37}$$

$$\frac{1}{r}\frac{\partial V}{\partial \theta} = \frac{dF}{dr} - ikU_\theta, \tag{38}$$

$$\frac{1}{r}\frac{\partial U_r}{\partial \theta} + \frac{\partial U_\theta}{\partial r} = i\,k\,F, \tag{39}$$

$$P = \frac{2}{r}\frac{\partial U_\theta}{\partial \theta} - \frac{1}{kCa}\left(\frac{d^2F}{dr^2} - k^2 F\right), \tag{40}$$

and

$$U_r = U_\theta = V = 0 \quad \text{at } \theta = 0. \tag{41}$$

We find that a suitable local asymptotic expansion, valid for $r \ll 1$, takes the form

$$U_\theta = U_{\theta 0}(\theta) + r\log r U_{\theta 1}(\theta) + rU_{\theta 2}(\theta) + \ldots,$$

$$U_r = U_{r0}(\theta) + \ldots,$$

$$V = r(\log r)^2 V_0(\theta) + r\log r V_1(\theta) + rV_2(\theta) + \ldots,$$

$$P = r^{-1}P_0(\theta) + \ldots,$$

$$F = F_0 + r\log r F_1 + rF_2 + \ldots$$

The nonintegrable singularity in the pressure as $r \to 0$ is a consequence of the moving contact line and the no slip boundary condition. If we substitute these expansions into (34) to (41), we can determine the functions of θ in the expansions. The key result is that

$$F \sim F(0)\left\{1 - i\,k\,c\frac{2}{\pi}\left(2 + \frac{\pi^2}{4}\right)Ca\,(r\log r + r)\right\} + ar \quad \text{as } r \to 0, \tag{42}$$

for some constant a.

Note that the slope of the contact line is of $O(\log r)$ as $r \to 0$. This is consistent with the results presented by Cox [6]. He showed that, if the capillary number is sufficiently small, the asymptotic solution given by (42) can be matched directly to an inner region where slip occurs. Since we are

pursuing a linear stability analysis, the capillary number associated with the velocity of the contact line (not Ca) is arbitrarily small, and Cox's two region asymptotic analysis applies here. If the size of the inner slip region is ϵ, we need

$$\frac{dF}{dr}(\epsilon) = 0,$$

and hence

$$a = \frac{2}{\pi}\left(2 + \frac{\pi^2}{4}\right) F(0)\, i\, k\, Ca\, c\, (\log\epsilon + 2)\,.$$

This means, noting that $r = x$ at $z = 0$, that

$$F \sim F(0)\left\{1 - i\, k\, c\frac{2}{\pi}\left(2 + \frac{\pi^2}{4}\right) Ca\, x\, (\log(x/\epsilon) - 1)\right\} \quad \text{as } x \to 0. \tag{43}$$

To find the analogous boundary condition near $x = 1$, we apply symmetry arguments on the map $x \to 1 - x$ and apply the same procedure above.

$$F \sim F(1)\left\{1 - i\, k\, c\frac{2}{\pi}\left(2 + \frac{\pi^2}{4}\right) Ca\ (1 - x)\, (\log((1 - x)/\epsilon) - 1)\right\} \quad \text{as } 1 - x \to 0. \tag{44}$$

These boundary conditions are the ones that we use instead of (33). In the following computations, we use $\epsilon = 10^{-5}$. The solution did not seem very sensitive to changes in ϵ in a few test cases that we tried.

3 Method and Results

We aim to solve the eigenvalue problem given by (23)-(32) and (43)-(44) using a finite difference discretisation of the governing equations. We begin by truncating the semi-infinite domain of solution to the rectangle $0 < x < 1$ and $-L < z < 0$, and choose $L > 0$ sufficiently large that the solution converges, replacing (28) with

$$U = V = W = 0 \quad \text{at } z = -L \text{ for } 0 < x < 1. \tag{45}$$

Secondly, we scale U, W, P on k, and consider the growth rate $\lambda = -ic$. Hence, if $\mathrm{Re}\,\{\lambda\} > 0$, then the base-state flow is unstable to this disturbance. In our results, we report in terms of growth rate ($\mathrm{Re}\{\lambda\}$) and the phase speed $\mathrm{Re}\{c\}$.

Since (23), (24) and (26), with $Re = 0$, are the two-dimensional Stokes equations with a source of mass due to the cross flow, we anticipate that we will need to use a staggered grid. We locate the discretised velocities, U, V and W, at the x-edges, centres and z-edges respectively of cells with corners $x = x_i$ for $i = 1, 2, \ldots, N$ and $z = z_j$ for $j = 1, 2, \ldots, M$, as shown in figure 2. We will not assume that the grid is uniform, but we will need $x_1 = 0$, $x_N = 1$, $z_1 = -L$ and $z_{M-1} + z_M = 0$. The discretised pressure is located at the centre of each cell, as is the discretised position of the free surface along the line $z = 0$. In addition, we require ghost points that lie outside the domain of solution, in order to be able to implement the boundary conditions. Specifically, we need ghost

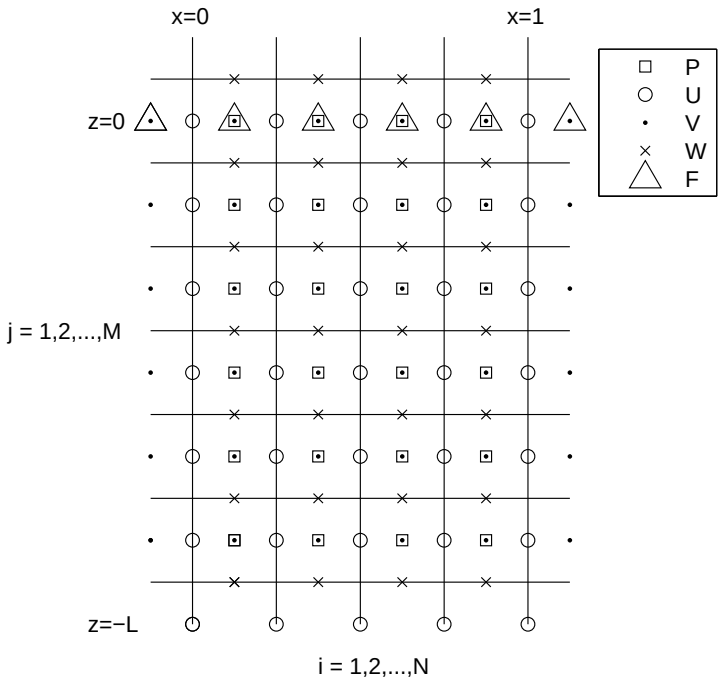

Figure 2: *The discretisation of the linear stability problem.*

values of F and V at the x-boundaries, ghost values of U at the boundary $z = -L$ and ghost values of W at the boundary $z = 0$. This is easy to see in figure 2.

With the unknowns discretised in this manner, it is straightforward to discretise the governing equations and boundary conditions. This gives us a set of linear equations that can be written in matrix-vector form as a generalized eigenvalue problem, $(A - \lambda B)y = 0$. We set up the matrices A and B in MATLAB in sparse form. For given k and Ca with $Re = 0$, we can calculate the eigenvalues, λ, and associated eigenvectors, y, very efficiently with the MATLAB routine `eigs`, which uses an iterative method (Cholesky factorization) optimized for sparse matrices. We restrict our disturbances in this paper to Stokes flow, since the matrix B cannot be written in symmetric form when $Re \neq 0$.

In the results shown below, we used a grid with spacing 10^{-3} in the x-direction close to the contact lines, increasing gradually to 10^{-2} away from the contact lines. In total, there are 130 cells in the x-direction. Similarly, in the z-direction, the grid spacing is 10^{-3} at the free surface, gradually increasing to 0.25 for larger z. We also found that we needed to reduce the z-grid spacing close to the boundary $z = -L$ to achieve a converged solution. In total, there are 143 cells in the z-direction. We performed several grid refinement tests to check that the solution had converged.

Figure 3 shows how the real and imaginary parts of the first few eigenvalues λ vary with k for $Ca = 1.5$. The eigenvalues and corresponding eigensolutions seem to be of two types.

Firstly, there is a sequence of eigenvalues with $\mathrm{Re}\{\lambda\} < 0$. These are stable eigenmodes that

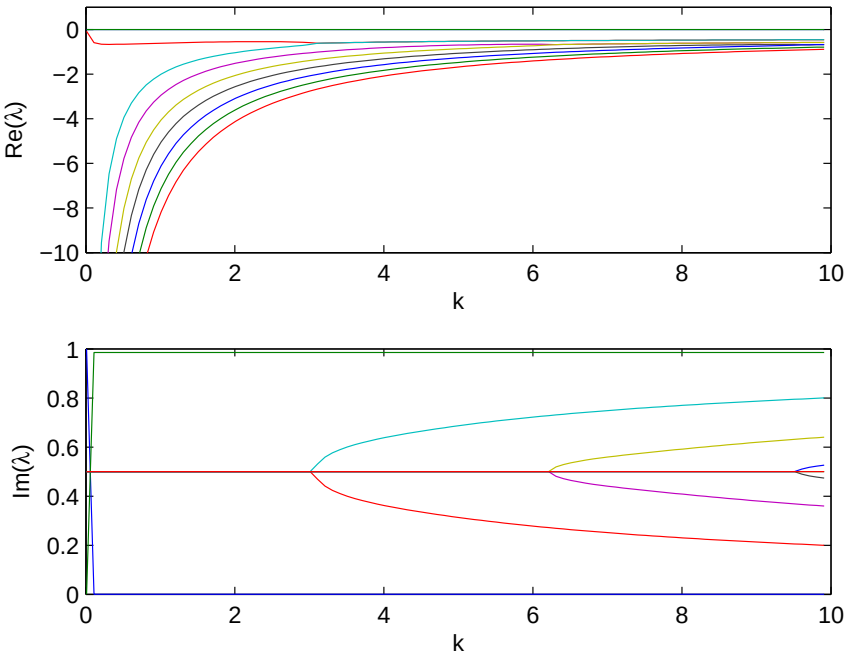

Figure 3: *The real and imaginary parts of the first 10 eigenvalues for* $Re = Ga = 0, Ca = 1.5$.

move at the mean value of the velocities of the walls ($\mathrm{Re}\{c\} = 1/2$) for $k < k_H \approx 3.1$. These stable eigenmodes then do not move with either wall, and decay exponentially with time. At $k = k_H$ there is a Hopf bifurcation. For $k > k_H$, the real parts of the first two stable eigenmodes become equal, and their imaginary parts deviate from $1/2$, which indicates the formation of an oscillatory mode. The behaviour of these modes corresponds to decaying standing waves in a frame of reference moving with the average of the plate velocities. We expect a sequence of such bifurcations as k increases. Some typical eigensolutions of this first type are shown in Figures 4.

Secondly, there are two neutral eigenmodes with zero real part, which are mirror images about the centre line, $x = 1/2$. These neither grow nor decay in this linear approximation. One mode has phase speed $\mathrm{Re}\{c\} = 0$ and the other $\mathrm{Re}\{c\} = 1$. When k is moderately large, each mode is localized at one of the walls, and moves with that wall (see Figure 5). For smaller values of k, the eigenmode does not look very different to the stable eigenmodes shown in Figures 6a and 6b. However, the key difference is that the neutrally-stable eigenmodes have a nonzero contact line displacement.

These eigenvalues for $k = 2\pi$ is shown in Figure 7. Again, the Hopf bifurcation is apparent as the capillary number is increased. Note that two different pairs of modes along the $\mathrm{Re}\{c\} = 1/2$ axis have undergone this transition when $Ca = 2$. In Figure 7 we show the least decaying modes in the typical interfacial shapes and the real and imaginary part of the velocity components.

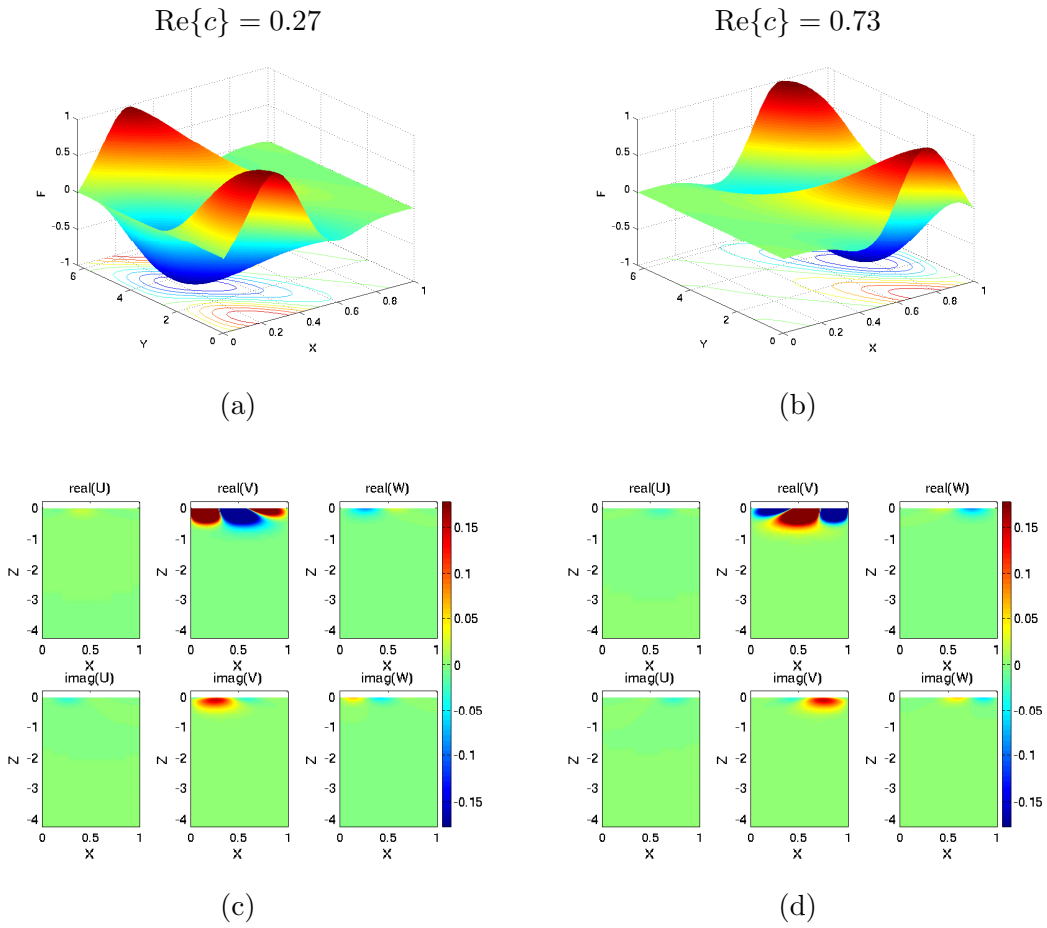

Figure 4: *(a,b): The free surface displacement of the least stable ($Re\{\lambda\} = -0.5$) stable eigenmodes for $Ca = 1.5$, $k = 2\pi$. (c,d) The real and imaginary parts of the eigenfunctions for the velocity field for the first two neutrally stable eigenvalues.*

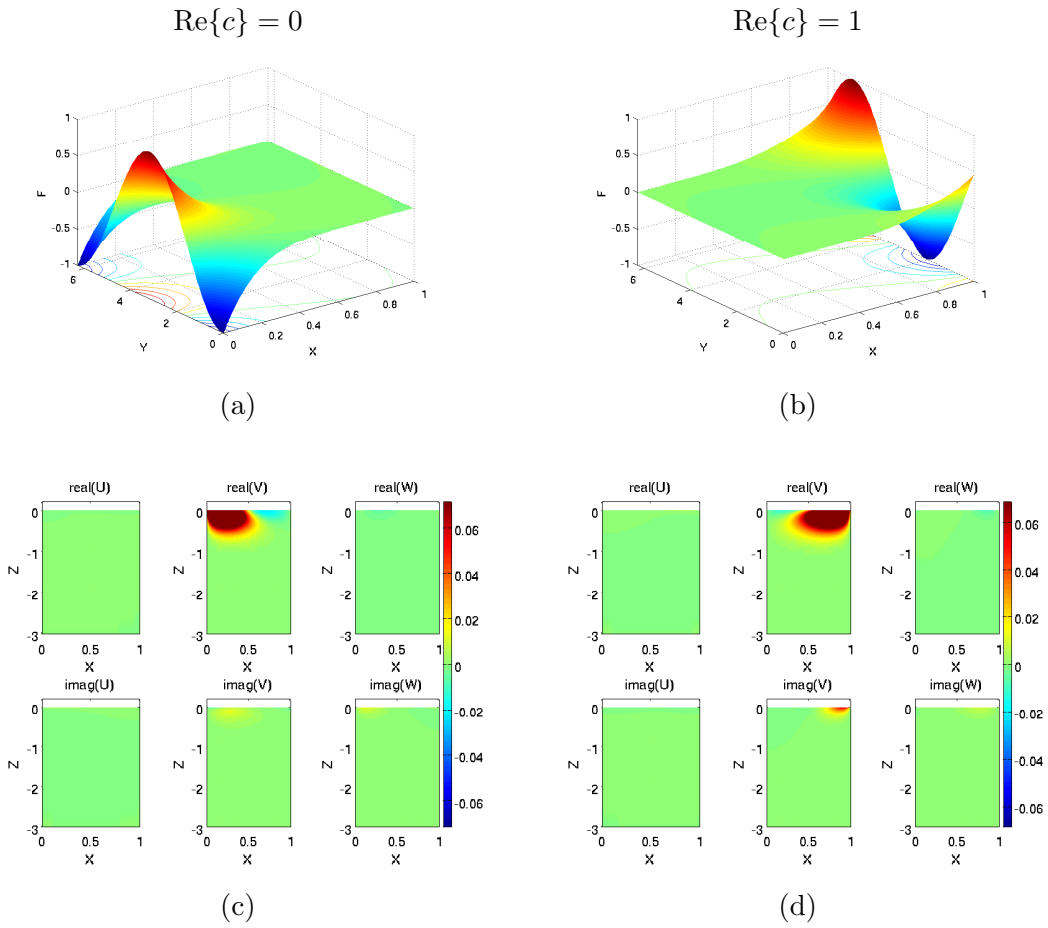

Figure 5: *(a,b): The free surface displacement of the first 2 neutrally stable eigenmodes for* $Ca = 1.5$, $k = 2\pi$. *(c,d) The real and imaginary parts of the eigenfunctions for the velocity field for the first 2 neutrally stable eigenvalues.*

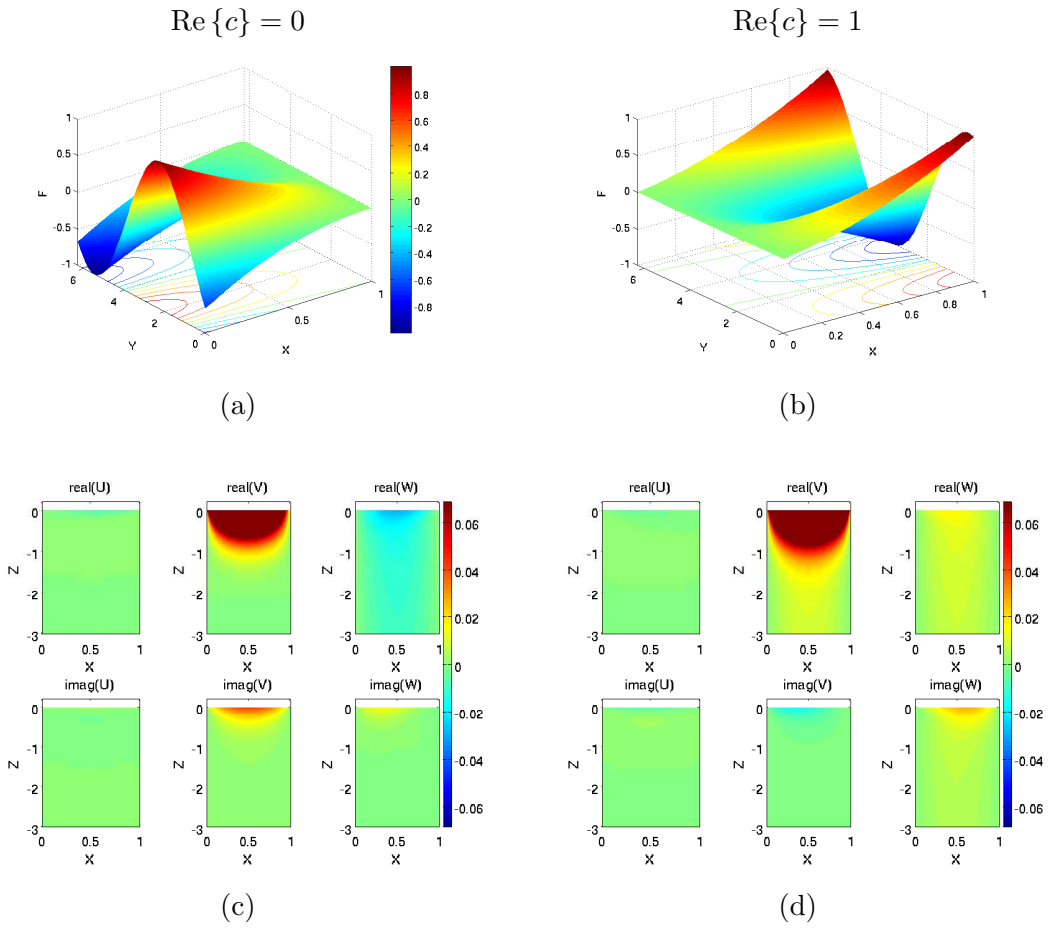

Figure 6: *(a,b): The free surface displacement of the first 2 neutrally stable eigenmodes for $Ca = 1.5$, $k = 0.1$. (c,d) The real and imaginary parts of the eigenfunctions for the velocity field for the first 2 neutrally stable eigenvalues.*

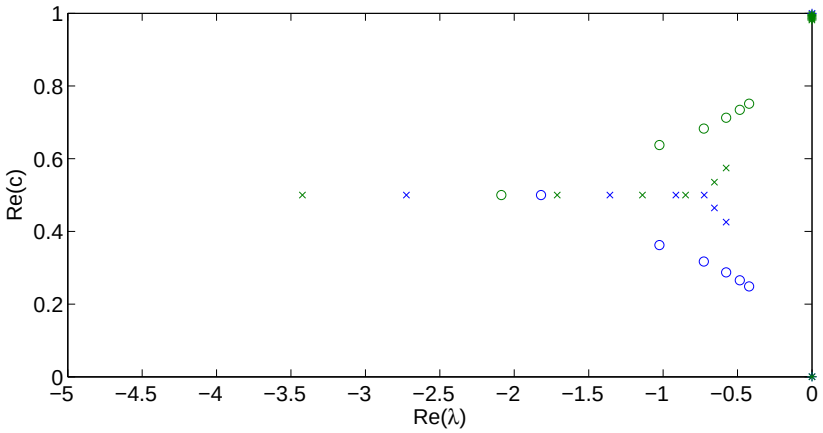

Figure 7: *The first 6 eigenvalues for* $0.01 < Ca < 2$ *with* $Re = Ga = 0, k = 2\pi$. *Neutral modes:* $*$, *First Hopf modes:* $\circ$, *Secondary Hopf modes:* $\times$.

4 Conclusions

In this paper, we investigated the linear stability of the meniscus region of a fluid-dynamic bearing of a hard disk drive. Previous inviscid results [2] reported an instability for the slot geometry when inertial effects dominate over capillary effects. Their assumption to keep $c_r = U_o/2$ fixed prescribes the assumption of a stationary wave in the frame moving with the average velocity whose amplitude grows with the growth rate. We found, in the limit when viscous effects dominate over inertial effects, including contact-line conditions at the gas-liquid-solid trijunctions, that the flat meniscus is stable. However, the least stable modes undergo a Hopf bifurcation which suggests that the disturbance appears as a *standing* wave moving with the mean speed $c_r = U_o/2$. Hence, it is not clear if these standing waves are the primary mode of instability for $Re \neq 0$. The nonzero Reynolds number problem is computationally more challenging, since Cholesky factorization cannot be applied to the discretised problem. We examine this case in a future work.

Acknowledgments

This industrial problem was presented at the Mathematical Problems in Industry Workshop in 2005 at Worcester Polytechnic Institute (WPI). We would also like to thank C.S. Raymond for his contributions to this work.

References

[1] W.C. Blount, *Fluid Dynamic Bearing Spindle Motors: Their future in hard disk drives*, IBM Corporation White Paper, IBM Storage Systems Group, San Jose, CA. 95193. 9

[2] J.S. Walker, G. Talmage, S.H. Brown, and N.A. Sondergaard, *Kelvin-Helmholtz instability of Couette flow between vertical walls with a free surface*, Physics of Fluids A, Volume 5 Issue 6, pp. 1468-1471 (1993). 10, 23

[3] F. Hendriks, B.S. Tilley, J. Billingham, P. Dellar, and R. Hinch, *Dynamics of the Oil-Air Interface in Hard Disk Drive Bearings*, IEEE Transactions on Magnetics, Volume 41 Issue 10, pp. 2884-2886 (2005). 10

[4] G.M. Homsy, *Viscous Fingering in Porous Media*, Annual Review of Fluid Mechanics, Volume 19, pp. 271-311 (1987). 10

[5] E.B. Dussan V. and S.H. Davis, *On the motion of a fluid-fluid interface along a solid surface*, Journal of Fluid Mechanics, Volume 65, pp. 71-95 (1974). 14

[6] R.G. Cox, *The dynamics of the spreading of liquids on a solid surface. Part I. Viscous flow.*, Journal of Fluid Mechanics, Volume 168, pp. 169-194 (1986). 14, 15